

Entanglement in Many-Body Fermion Systems

Michelle Storms^{1,2}

¹*Department of Physics, University of California Davis, CA 95616, USA*

²*Department of Physics and Astronomy, Ohio Wesleyan University, Delaware, OH 43015, USA*

(Dated: January 14, 2014)

The present study examines the quantum entanglement in several bipartite fermion lattices, with various Fermi surfaces and a staggered chemical potential. In ground state systems, the entanglement scales as the area of the boundary between the two regions, and the coefficient of this line term was found to vary logarithmically with the staggered potential. Furthermore, this relation is governed by the geometry of the Fermi surface of the lattice, as evidenced by results in the pi-flux and anisotropic cases. In addition, the entanglement entropy of excited state systems was found to scale as the volume of the system. When examined as a function of energy, the entanglement entropy of the excited state systems was found to approach expected behavior only as the two parts of the bipartite lattice become severely unequal in size.

INTRODUCTION

Quantum entanglement, a phenomenon Schrödinger referred to as “*the characteristic trait of quantum mechanics*”[1], has recently been of great interest to the physics community. With applications in computing, encryption, and communication, it is worth examining quantum entanglement not only in two or three particle systems, but also in large lattices of entangled particles. Here we find that quantum entanglement, and the related measure of entanglement entropy, are related to some of the most fundamental concepts in our understanding of condensed matter physics.

Von Neumann entanglement entropy is a simple extension of information entropy in bipartite lattices of entangled particles. Entropy is used as a logarithmic measure of entanglement between two halves of a system. The entanglement entropy of ground state systems is a subject of great interest, and is known to scale as the “area” of the boundary between the two regions for systems with an energy gap. This “area-law” behavior was first discovered in the context of classical information transfer in black hole physics [2][3], and has since extended to quantum entanglement entropy. While the Hilbert space for a many-body system scales exponentially with the volume of the system, rendering calculations impractical, this counter-intuitive area-law property of the ground state allows for calculations involving many-body systems via methods like the density matrix renormalization group (DMRG) [4]. The present study seeks to confirm this basic area-law relation in one-, two-, and three-dimensional systems, with several variations on the basic model. For more details concerning the current study, see [5].

An interesting extension of the model is to examine a gapped system, achieved in our model via a staggered chemical potential μ_s , and its behavior as the system becomes gapless ($\mu_s \rightarrow 0$). The area law line term, *i.e.* the coefficient of the linear term in the expression for $s_{VN}(N)$, is expected to vary logarithmically with μ_s for sufficiently large system sizes and sufficiently small values of μ_s . In addition to these gaps, we also examine the effect of Fermi surface geometry on the behavior of this divergence.

Systems in excited states display instead a “volume-law”, that is, the entropy scales instead with the volume of the system. While this relation offers no computational benefits to exploit, it does allow for the examination of entropy as a function of energy (*i.e.* the entropy density function), which is well-understood for information entropy. We shall determine to what extent the entanglement entropy density function calculated using these exact methods agrees with the thermodynamic entropy density function obtained from statistical mechanics. Agreement indicates that our lattice can be treated as a “particle in a heat bath”, and thus described using statistical physics.

METHODS

Tight-Binding Model

Our model involved a bipartite square lattice of atoms with one spinless electron either present or not present in the valence shell. Because the model disregards the spin of the electron, a maximum of one electron can occupy a lattice site at any given time. The lattice had periodic boundary conditions, and we considered the two halves such that no corner terms were introduced into our calculation. We used the tight-binding model Hamiltonian

$$\mathcal{H} = \sum_{\langle i,j \rangle} t_{i,j} (c_i^\dagger c_j + c_j^\dagger c_i) + \mu_s \sum_i (-1)^i n_i. \quad (1)$$

where the creation and destruction operators (c_i^\dagger and c_i respectively) represent a particle being created or destroyed at lattice site i . Thus the first term in Eq. 1 represents the possibility of an electron moving between nearest neighbor lattice sites with a coefficient $t_{i,j}$ called the transfer integral. The basic model is isotropic in the transfer integral, but we also examine the anisotropic case with distinct transfer integrals in each direction, and define $q = \frac{t_x}{t_y}$. This changes the Fermi surface of the lattice, as seen in Fig. 1. Furthermore, each atom has a constant chemical potential μ_c , which does not factor into the Hamiltonian, and the lattice includes a staggered chemical po-

tential μ_s on alternating atoms, which serves to create a gap in the energy spectrum of the lattice (see Fig.2). This staggered chemical potential is represented by the second term in Eq. 1, where n_i is an operator equivalent to $c_i^\dagger c_i$ and thus serves to “count” the number of particles present on a particular lattice site. See Fig. 3 for a summary of the lattice arrangement.

In addition to the above zero-flux case, we examine a pi-flux potential in two dimensions. Here, the sign of alternating transfer integrals are switched, as in Fig.4. This potential is derived from Mean Field Theory models of superconductivity and can be modeled as an extremely large magnetic field passing through the lattice [6]. The pi-flux case is fundamentally different from the zero-flux case, as it exhibits a point Fermi surface (see Fig. 1), and a Dirac energy spectrum (see Fig. 2).

It is necessary to work with Eq. 1 in momentum space and exploit lattice symmetries to diagonalize the Hamiltonian. Once diagonalized, the Hamiltonian is of the form

$$\mathcal{H} = \sum_{\vec{k}} [\epsilon_{-}(\vec{k})\alpha_k^\dagger\alpha_k + \epsilon_{+}(\vec{k})\beta_k^\dagger\beta_k] \quad (2)$$

where, for a ground state system with twice as many sites as electrons, $\langle\alpha_k^\dagger\alpha_k\rangle = 1$ and $\langle\beta_k^\dagger\beta_k\rangle = 0$. Thus the ground state, half-filled system corresponds to the lower energy band being completely full and the upper energy band being completely empty. For the excited state calculations, both $\langle\alpha_k^\dagger\alpha_k\rangle$ and $\langle\beta_k^\dagger\beta_k\rangle$ can take values of 0 or 1, since the upper energy band is not necessarily empty. For this case, a program was created which assigned each of N electrons to one of $2N$ possible states. In this way, for a particular pair of (k_x, k_y) values, an electron could fill both, neither, or one of the lower or upper energy states. In order to sample a large range of system energies, it was possible to bias the assignment of states such that a particular percentage of electrons would be placed in the lower or upper energy band.

Correlation Matrix Method

We work primarily with the Von Neumann entanglement entropy, which is defined in terms of the reduced density matrix, ρ_A , for one part (labeled part A) of the bipartite lattice. The reduced density matrix is easily obtained from the full density matrix of the system by tracing out the degrees of freedom associated with the other part of the lattice (part B):

$$\rho_A = \text{Tr}_B(\rho) = \text{Tr}_B(|\Psi\rangle\langle\Psi|) \quad (3)$$

where Ψ is the wavefunction describing the entire lattice in its ground state. The Von Neumann entanglement entropy is then

$$s_{VN} = -\ln[\text{Tr}(\rho_A \ln \rho_A)]. \quad (4)$$

For non-interacting models, we can reformulate Eq. 4 in terms of the eigenvalues of a correlation matrix [7], defined to be

$$C_{i,j} = \langle c_i^\dagger c_j \rangle \quad (5)$$

where c_i^\dagger and c_j must be expressed in terms of $\alpha_k, \alpha_k^\dagger, \beta_k,$ and β_k^\dagger such that the matrix is scalar, real, and symmetric. The correlation matrix can be easily diagonalized by a conversion to tridiagonal, then diagonal form [8]. Once the eigenvalues λ_i of the correlation matrix have been obtained, Eq. 4 can be reformulated as

$$s_{VN} = \sum_i \lambda_i \ln(\lambda_i) + (1 - \lambda_i) \ln(1 - \lambda_i). \quad (6)$$

In general, the full correlation matrix grows as N^d for a system of linear size N and dimension d , making even two-dimensional systems impractical to diagonalize for large system sizes. However, if the broken symmetry is restricted to one spatial direction, *i.e.* the lattice is split only along the x, y, or z direction, the correlation matrix becomes block diagonal, with each block having order N . Each block can then be diagonalized separately and the block eigenvalues can be used directly in Eq. 6. The density matrix described above grows exponentially with the system size, so it is only using the correlation matrix that we may examine system sizes larger than a chain of six atoms. However, calculations were made using both methods in linear chains of four and six atoms to ensure that both methods gave the same results.

RESULTS

Area Law

The area law was found to be satisfied with each ground state system (see Fig. 5), with a line term coefficient varying with μ , according to Fig. 6. For the zero-flux one-, two-, and three-dimensional case, the dependence on $\ln(\frac{t}{\mu})$ becomes linear as the system approaches the gapless case (small μ). For the pi-flux case, however, we observe the line term approaching a constant value as a result of the point Fermi surface for this lattice.

Anisotropies

Because the anisotropy in the transfer integral changes the Fermi surface of the lattice, it is expected that the line term will vary not only with μ but also with the transfer integral ratio q . The line terms for several different q values were plotted against $\ln(\frac{t}{\mu})$, where $t_y = t$ and $t_x = qt$. A fit was made to the linear region of these plots (see Fig. 7). The slope (normalized to $q = 1$) of this linear region was found to vary with q according to the Widom Conjecture [9] (see Fig. 8), with better fits for $q < 1$. It is hypothesized that for $q > 1$, the system size was insufficient to give an accurate representation of the system’s behavior for small μ .

Excited States

As expected, the excited state entropies were found to scale as the volume of the system. Figure 9 represents several states near maximum entropy, where the electrons are split nearly equally between the two energy bands. The entanglement entropy was found to vary only slightly among randomly-generated states with the same energy. Examined as a function of the system energy (see Fig. 10), it was discovered that the entanglement entropy for our basic bipartite lattice was consistently less than the thermodynamic entropy calculated for the system, both with finite and infinite system size. However, upon reducing the ratio of the sizes of the two parts of the lattice from our original 1:1 ratio, we found that the system approaches agreement with the statistical prediction. Figure 11 demonstrates the effect of considering a part of the lattice that is $1/2$, $1/4$, $1/5$, $1/10$, and $1/20$ of the entire lattice. As the examined lattice part becomes smaller in size, it can more accurately be modeled as the "particle and heat bath" necessary for the assumptions of statistical mechanics.

CONCLUSIONS AND FURTHER WORK

We have demonstrated the area-law scaling of entanglement entropy in one-, two-, and three-dimensional fermion lattices. Furthermore, we have demonstrated the relationship between this area-law line term and the staggered chemical potential μ_s , which is fundamentally related to the gap in the energy spectrum of the lattice. This relationship is also dependent on the geometry of the Fermi Surface for a particular lattice. This is demonstrated in both the pi-flux case, where the dependence on μ_s saturates to a constant value, and in the anisotropic case, where the dependence on μ_s appears to scale according to the Widom Conjecture. In our examination of excited states, we demonstrated a volume-law entropy scaling, as well as an entropy density function that is significantly reduced from the known thermodynamic entropy density function for equally-sized parts of the bipartite lattice. This entanglement entropy

density function approaches the thermodynamic entropy density function as we examine a smaller and smaller part of the bipartite lattice, integrating out the majority of the lattice.

A simple but interesting extension of our model would be to divide our system into a regions with corners. This would have the effect of adding a constant corner term to the entropy. The behavior of this corner term can also be examined as $\mu_s \rightarrow 0$. A more complicated examination of the concepts proposed in the current study would be to calculate the entanglement entropies for interacting models with small system sizes. Although this would introduce significant finite size effects, it would also give information about the difference in the equilibrium states of non-integrable and integrable models, and how these differences affect the calculated value of entanglement entropy.

ACKNOWLEDGMENTS

I thank Rajiv R.P. Singh for his mentorship and collaboration on this research. This work is supported by NSF REU grant number 1263201.

-
- [1] E. Schrödinger (1935). Discussion of Probability Relations between Separated Systems. *Mathematical Proceedings of the Cambridge Philosophical Society*, 31, pp 555-563. doi:10.1017/S0305004100013554.
 - [2] T. M. Fiola, J. Preskill, A. Strominger, and S. P. Trivedi, *Phys. Rev. D* 50, 3987 (1994).
 - [3] C. Holzhey, F. Larsen, and F. Wilczek, *Nucl. Phys. B* 424, 443 (1994).
 - [4] U. Schollwöck, *Rev. Mod. Phys.* 77 259 (2005).
 - [5] M. Storms, R.R.P. Singh, cond-mat arXiv:1308.6257v2.
 - [6] J.B. Marston and I. Affleck, *Phys. Rev. B* 39, 11538 (1989).
 - [7] I. Peschel and V. Eisler, *J. Phys. A-Math. and Theor.* 42, 504003 (2009).
 - [8] W.H. Press, S.A. Teukolsky, W.T. Vetterling, B.P. Flannery, *Numerical Recipes in Fortran 77* (Cambridge University Press, New York, NY, 1992).
 - [9] D. Gioev and I. Klich, *Phys. Rev. Lett.* 96, 100503 (2006).

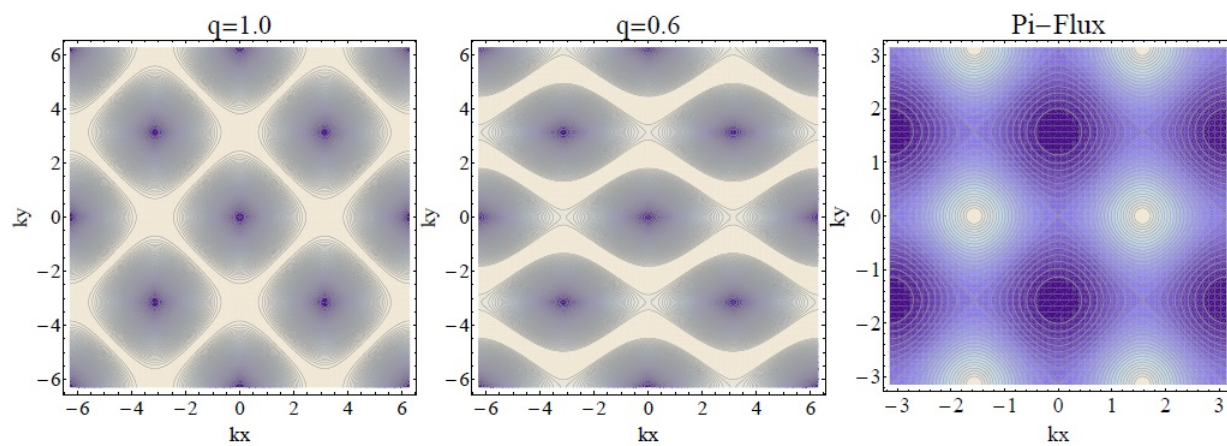


FIG. 1: Fermi Surface

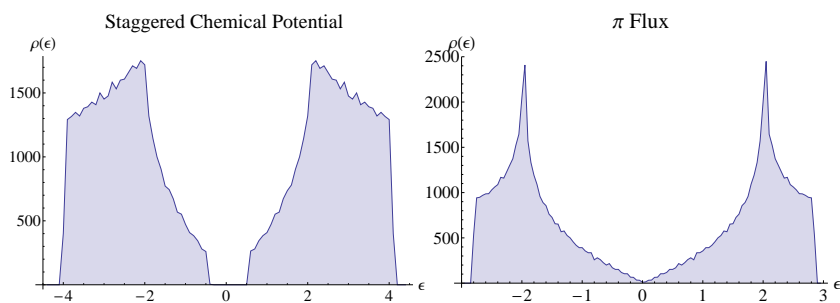


FIG. 2: Density of States

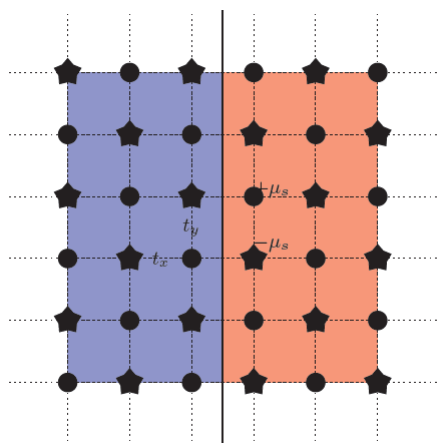


FIG. 3: Staggered Chemical Potential: Alternating lattice sites are held at different potentials, transfer integrals in the x and y directions are independent.

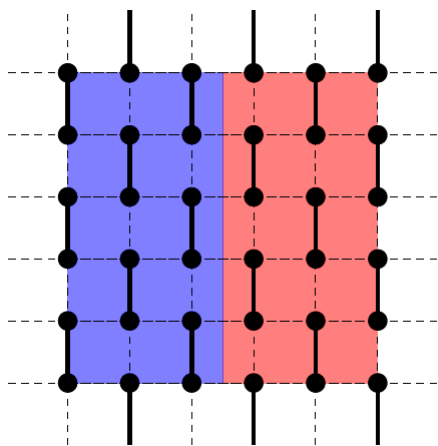


FIG. 4: Pi-Flux: Bold lines indicate a negative transfer integral, dotted lines represent a positive transfer integral.

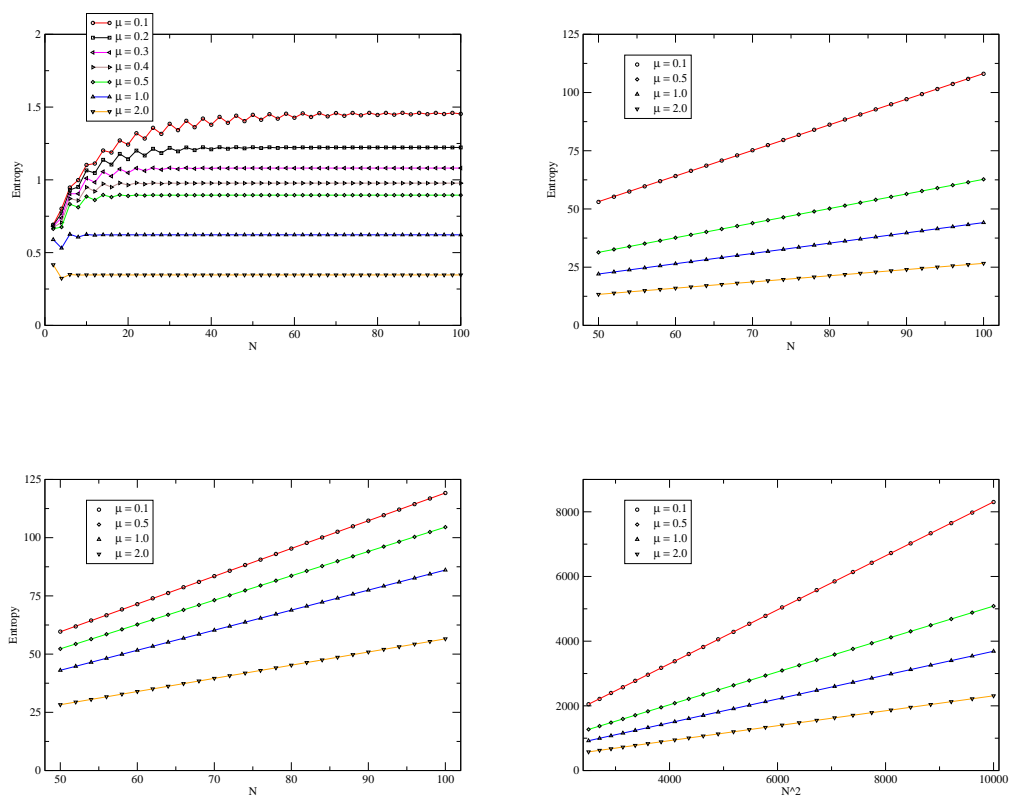


FIG. 5: Area Law, using 1D lattice (top left), 2D lattice (top right), 2D lattice with Pi-Flux potential (bottom left) and 3D lattice (bottom right)

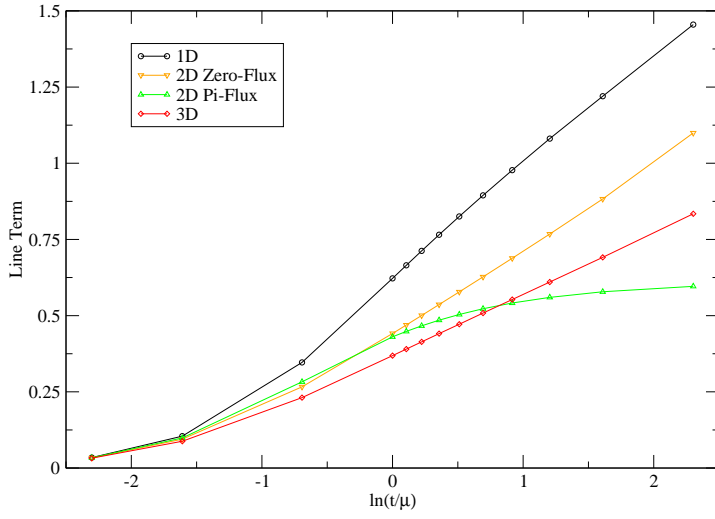


FIG. 6: Line terms by dimension

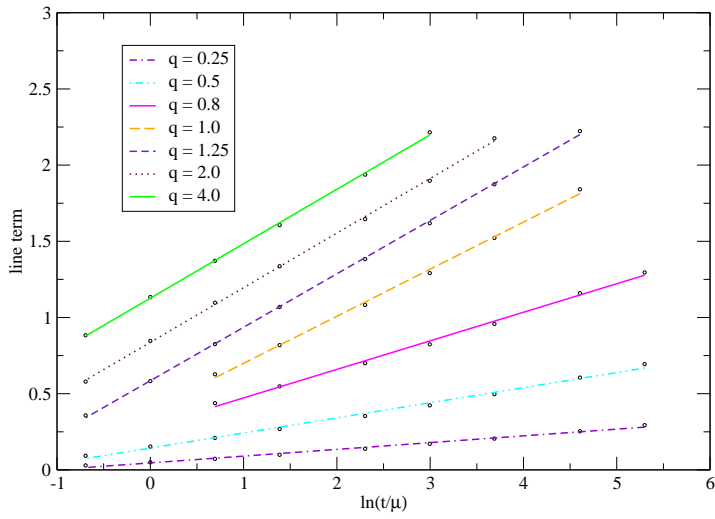


FIG. 7: Line terms for different q values

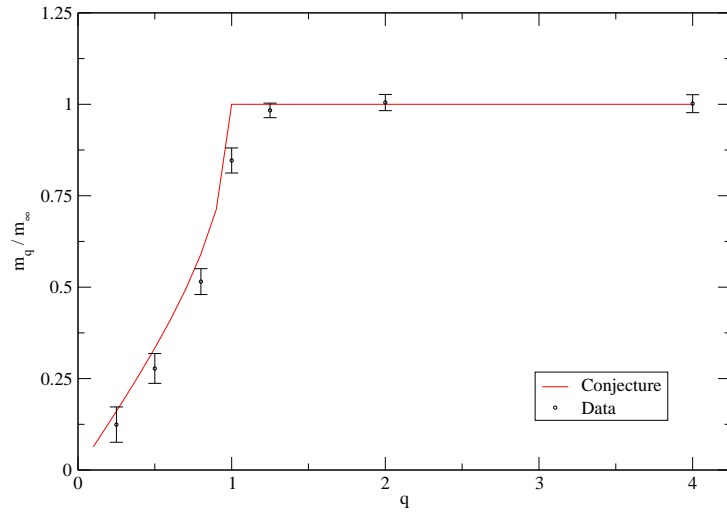


FIG. 8: Widom Conjecture

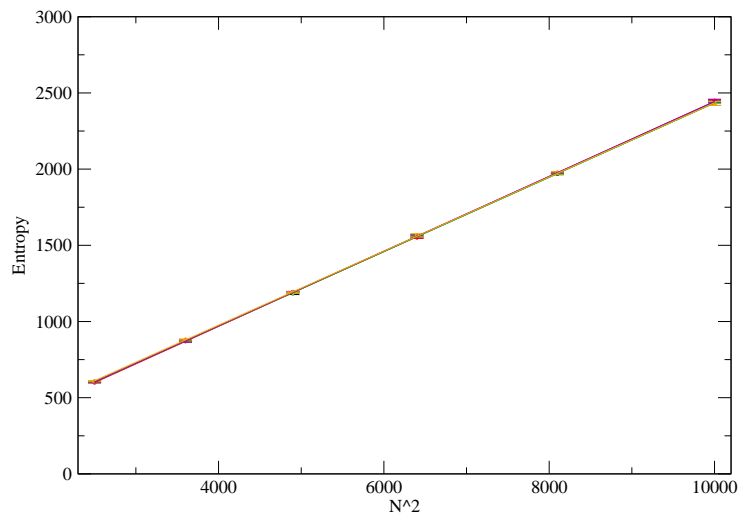


FIG. 9: Excited States

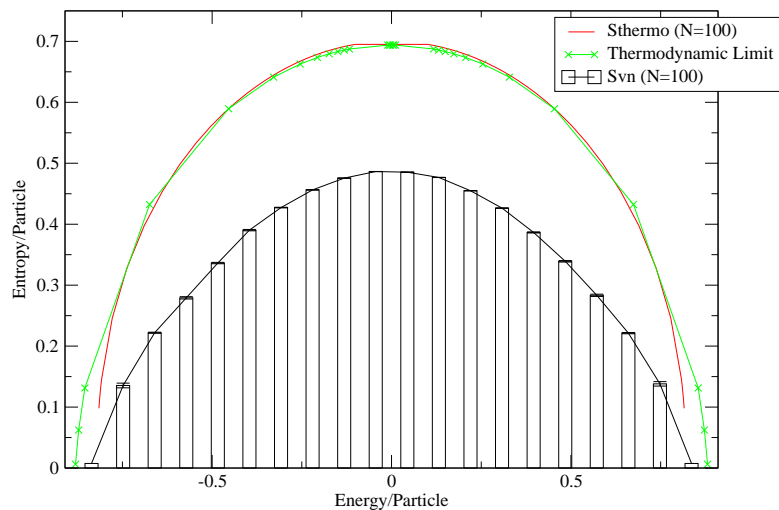


FIG. 10: Entanglement Entropy Density Function for 1:1 Ratio

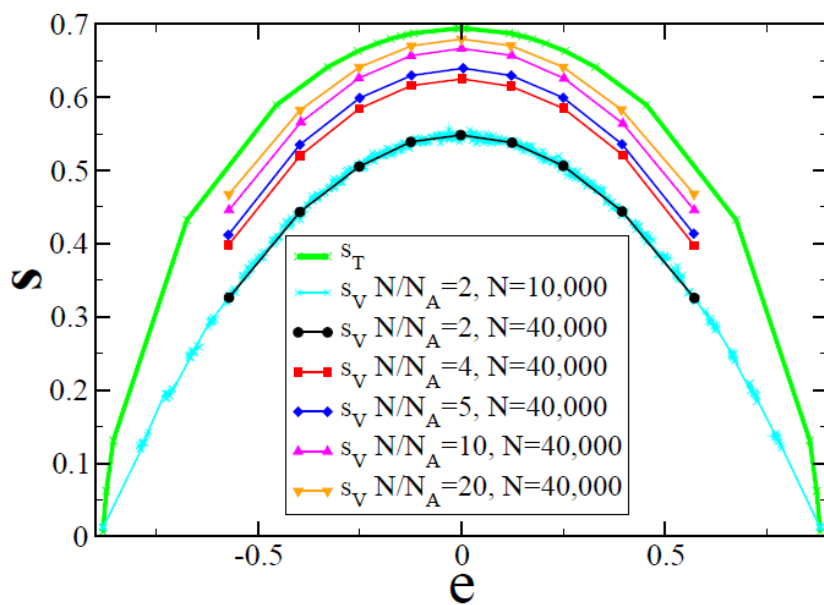


FIG. 11: Entanglement Entropy Density Function for Various Ratios